Department of Mathematics and Statistics

Preprint MPCS-2018-07

5 October 2018

M.J. Baines

A two-phase moving mesh finite element model of segregated competition-diffusion

A. R. Watkins and M. J. Baines

Department of Mathematics and Statistics, University of Reading,
P.O.Box 220, Reading, RG6 6AX, UK

Abstract

A finite element numerical solution of the Lotka-Volterra competition-diffusion model of theoretical ecology is presented which depends on a conservation-based moving mesh. The model parameters are chosen such that the competition is strong enough to spatially segregate the two populations, leading to a two-phase problem with a coupling condition at the moving interface. Incorporation of the moving interface into the finite element solution preserves the identities of the two species in space and time, enabling parameters to be referred to each separate population as the interface moves.

1 Introduction

We consider the application of a conservation-based moving mesh finite element method [1, 3] to a model of population dynamics. A version of the Lotka-Volterra competition model is taken that describes a two-phase segregated reaction-diffusion system and the moving mesh method implemented for this system. We examine a two-phase Lotka-Volterra competition-diffusion system with a high competition limit, so that the species are completely spatially segregated and interact only though their interface using an interface condition based on this high competition limit [4, 6].

The model is implemented numerically with a variety of creative parameter combinations, and various behaviours are observed which dominate in turn as the populations evolve through time.

It is shown in [4] that where competition is strong enough to spatially segregate two populations the Lotka-Volterra PDE system can be reduced to a form similar to a Stefan problem, The Stefan problem has been considered numerically in [2] usiing a moving mesh finite element method based on conservation (MMFEM). The two major differences between the Stefan model and the Lotka-Volterra model are, firstly, there are additional logistic growth terms in the Lotka-Volterra model, and secondly, there is a parameter in the Lotka-Volterra model of the interface (the equivalent of the latent heat coefficient of the Stefan problem) which is set equal to zero. In biological terms, one species does not transform into another, which means that unlike the Stefan problem the competition system has an interface condition that does not specify an interface velocity. This presents a challenge when attempting to apply the same approach to the Lotka-Volterra model as to the Stefan problem in [2] because that paper uses the interface velocity taken directly from that condition.

However, the moving mesh finite element method approach in [2] is a promising way to model the competition system because it not only directly tracks the evolution of the interface between species, it provides a framework for keeping particular mesh nodes attached to particular species. This means that the internal dynamics of a species can be assigned to particular nodes or elements rather than particular parts of space, and the dynamics for any given location will automatically be those of the correct species.

In this paper we model, in one dimension, the system described by Hilhorst *et al.* [4] using a moving mesh finite element method (MMFEM) developed from that in [2]. We demonstrate that the MMFEM method can be extended to include logistic growth terms and also applied to problems

$$\frac{\partial u_2}{\partial t} = {}_2\frac{\partial^2 u_2}{\partial x^2} + g(u_1; u_2)u_2 \qquad x \in R_2(t) \quad t > 0 \tag{2}$$

where ${}_1$, ${}_2$ are constant diffusion coefficients and with (in general)

$$f(u_1$$

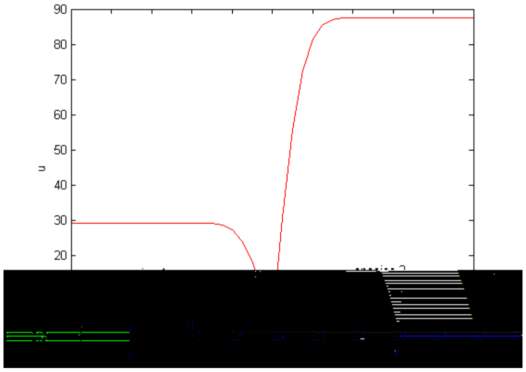

Figure 1: Initial conditions for the competition system, with population density U_1 of species 1 (on the left) and U_2 of species 2 (on the right). The interface node has zero population and must always satisfy the interface condition.

interface and annihilate each other in a ratio determined by the competition coefficient . This condition is given in [4] as

$$ {}_1\frac{\partial u_1}{\partial x} = \quad {}_2\frac{\partial u_2}{\partial x} \tag{5}$$

where $= K_2/K_1$. We call the interspecies competition rate. Because the annihilation is complete we also have a zero Dirichlet condition,

$$u_1 = u_2 = 0;$$

at the interface. Zero Neumann boundary conditions $\partial u_1/\partial x = 0$ and $\partial u_2/\partial x = 0$ are applied at fixed external boundaries away from the interface.

Initial conditions on u_1 and u_2 are not given in [4], but we select suitable initial conditions and physical parameters such that one species is in growth and the other in decline. The initial conditions are shown in figure (1).

3 The MMFEM conservation method

3.1 Weak forms

We begin by writing the governing Lotka-Volterra equations (3) and (4) in the weak forms

$$\int_{R_p(t)} w(x;t)\frac{\partial u_p}{\partial t}\mathrm{d}x = {}_p \int_{R_p(t)} w(x;t)\frac{\partial^2 u_p}{\partial x^2}\mathrm{d}x + r_p \int_{R_p(t)} w(x;t)\, u_p \quad 1 \quad \frac{u_1}{k_1} \quad \mathrm{d}x; \tag{6}$$

$(p = 1; 2)$, where $w(x;t)$ is a positive test function.

3.2 A relative conservation principle

The total population of each species is defined as ${}_p$, given by

$${}_p(t) = \int_{R_p(t)} u_p(x;t)\,\mathrm{d}x \tag{7}$$

$(p = 1; 2)$, where $R_p(t)$ is the domain inhabited by that species.

where $v_p(x;t)$ is the domain velocity. We suppose that the test function $w(x;t)$ moves with the velocity $v_p(x;t)$ induced by (8), so that

$$\frac{\partial w}{\partial t} + v_p\frac{\partial w}{\partial x} = 0$$

Hence (10) becomes

$$\frac{\mathrm{d}}{\mathrm{d}t}\left[\int_{R_p(t)} w(x;t)u_p(x;t)\mathrm{d}x\right] = \int_{R_p(t)} w(x;t)\frac{\partial}{\partial x}(u_pv_p\mathrm{d}x \quad \int_{R_p(t)} w(x;t)\frac{\partial u_p}{\partial t}\mathrm{d}x.$$

Therefore, by (9), the velocity v_p and rate of change of the total mass $\dot{\theta}_p$ in each region are given in terms of the constants c_p by

$$c_p\dot{\theta}_p\int_{R_p(t)} w(x;t)\frac{\partial}{\partial x}(u_p\underline{x}_p)\mathrm{d}x = \int_{R_p(t)} w(x;t)\frac{\partial u_p}{\partial t}\mathrm{d}x; \qquad (p = 1;2). \quad (11)$$

The boundary conditions have yet to be applied.

3.3 A velocity potential

At this point it is convenient to introduce a velocity potential ϕ_p, defined by

$$v_p = \frac{\partial \phi_p}{\partial x} \qquad (12)$$

so that equation (11) becomes

$$c_p\dot{\theta}_p\int_{R_p(t)} w(x;t)\frac{\partial}{\partial x}\left(u_p\frac{\partial \phi_p}{\partial x}\right)\mathrm{d}x = \int_{R_p(t)} w(x;t)\frac{\partial u_p}{\partial t}\mathrm{d}x;$$

for each species, or after integration by parts,

$$c_p\dot{\theta}_p\left[wu_p\frac{\partial \phi_p}{\partial x}\right]_{\partial R_p(t)} + \int_{R_p(t)} u_p(x;t)\,\frac{\partial w}{\partial x}\frac{\partial \phi_p}{\partial x}\mathrm{d}x = \int_{R_p(t)} w(x;t)\frac{\partial u_p}{\partial t}\mathrm{d}x. \quad (13)$$

3.4 Substituting the Lotka-Volterra equations

We now substitute the weak form of the governing PDEs (6) into the right hand side of (13), giving after a further integration by parts,

$$D_p\left[w\frac{\partial u_p}{\partial x}\right]_{\partial R_p(t)} \quad D_p\int_{R_p(t)}\frac{\partial w}{\partial x}\frac{\partial u_p}{\partial x}\mathrm{d}x + r_p\int_{R_p(t)} w(x;t)u_p(x;t)\left(1 - \frac{u_p(x;t)}{k_p}\right)\mathrm{d}x.$$

At the external boundaries @u_p=@x = 0 and also *v552 Tf 66.789 0 Td e (u)]Tnd x*

Moreover, the Stefan condition refers to a situation where the gradients of u either side of the interface are of the same sign in general. In contrast, equation (5) refers to an interface where the gradients either side are of opposite polarity, since $u = 0$ on the interface and the method requires positive populations, i.e. we have interfaces with 'V' shaped functions.

Whilst the interface velocity is not given explicitly by (5) the expression does contain information about the location of the interface implicitly. Thus, if we know $@u{=}@x$ in the interior of each region adjacent to the interface, we may use the fact that $u = 0$ at the interface to infer an interface position. We therefore seek an interface position such that the values of $@u{=}@x$ either side of the interface are in the ratio .

3.5.1 Approximating the interface condition

We shall adopt an explicit time-stepping approach which allows us to update the species and the interface simultaneously, but only to first order in time and subject to stability limitations on the time step. Should there be a problem in this regard, a suitable alternative would be to use an implicit time integration scheme, which would accord the ability to reassign the interface position.

At any given time t we approximate the interface condition (5) in the finite difference form

$$_1\frac{u_{1;m} \quad u_{1;m\quad 1}}{x_m \quad x_{m\quad 1}} = \quad {}_2\frac{u_{2;m+1} \quad u_{2;m}}{x_{m+1} \quad x_m};$$

where the subscript m denotes the interface node and the $x_i; u_{p;i}$, $(i = m \quad 1; m; m+1); (p = 1; 2);$ are adjacent node positions and solution values. Since $u_m = 0$ we obtain an expression for the position of the interface node x_m in terms of adjacent nodal values at $m \quad 1$ as

$$x_m = \quad {}_1u_{1;m} \quad {}_1x_{m+1} + \quad {}_2u_{2;m+1}x_{m\quad 1} \; {}_{+1}$$

ah Tf 11.76217.1971.95.76217.577.97

where t is the time step.

3.6 Finite elements and modified basis functions

We now consider spatial approximation of the velocities of the species in the two phases. Let the regions $R_1(t) = [0, x_m(t)]$ and $R_2(t) = [x_m(t), 1]$, where $x_m(t)$ is the position of the interface. Define the mesh

$$0 = X_0 < X_1(t) < \ldots < X_m(t) < \ldots < X_N(t) < X_{N+1} = 1$$

and choose the test function $w(x,t)$ to be a member of the set $\{W\}$ of standard piecewise-linear positive basis functions W_i $(0 < i < N+1)$ appropriate to Neumann boundary conditions, except for W_{m-1}, W_m, W_{m+1}. With the known value of the population at the interface node $X_m(t)$ in mind we discard the test function W_m and augment the adjacent test functions W_{m-1}, W_{m+1} by those parts of W_m lying in the relevant phase. The resulting set of test functions, $\{\tilde{W}_i\}$ say, called modified test functions in [5, 6], form a partition of unity in each phase.

The population densities u_p in each phase are now approximated by piecewise-linear functions U_p, $(p = 1, 2)$, projections of u_p into the spaces spanned by the $\{\tilde{W}_i\}$.

The total populations in the two phases are then

$$_1(t) = \int_0^{X_m(t)} U(x,t)\,\mathrm{d}x, \qquad _2(t) = \int_{X_m(t)}^{1} U(x,t)\,\mathrm{d}x \tag{18}$$

and the relative conservation principles in the two phases are

$$\frac{1}{_1(t)} \int_0^{X_m(t)} W_i\, U_1(x,t)\,\mathrm{d}x = c_{1,i}, \qquad \frac{1}{_2(t)} \int_{X_m(t)}^{1} W_i\, U_2(x,t)\,\mathrm{d}x = c_{2,i}.$$

where the constant-in-time partial populations $c_{1,i}$ and $c_{2,i}$ are obtained from (8) and the initial conditions at $t = 0$, giving

$$c_{1,i} = \frac{1}{_1(0)} \int_0^{X_m(0)} \tilde{W}_i(x,0) U_1(x,0)\mathrm{d}x, \quad c_{2,i} = \frac{1}{_2(0)} \int_{X_m(0)}^{1} \tilde{W}_i(x,0) U_2(x,0)\mathrm{d}x.$$

Note that due to the construction of the $\tilde{W}_i$ both $\sum_{i=0}^{m-1} c_{1,i}$ and $\sum_{i=m+1}^{N+1} c_{2,i}$ are equal to unity.

3.6.1 The finite element velocity potentials

We now substitute piecewise-linear finite element functions ${}_1; {}_2$ for ${}_1; {}_2$ into (14) to obtain, in phase 1,

$$\int_0^{X_m(t)} U_1(x;t)\,\frac{\partial \hat{W}_i}{\partial x}\,\frac{\partial {}_1}{\partial x}\,dx = c_{1;i} - 1 \quad {}_1 \int_0^{X_m(t)} \frac{\partial \hat{W}_i}{\partial x}\,\frac{\partial U_1}{\partial x}\,dx + {}_1 \quad W_i\,\frac{\partial U_1}{\partial x} \quad {}_{m(t)}$$

$$+\, r_1 \int_0^{X_m(t)} \hat{W}_i(x;t)\,U_1(x;t) \quad 1 \quad \frac{U_1(x;t)}{k_1} \quad dx; \qquad (i ==$$

$X_{m(t0)}$ $\hat{W}_1$ ∂

w_i

∂x

weak forms

$$\int_0^{X_m(t)} \tilde{W}_i(x;t)V_1(x;t)\,\mathrm{d}x = \int_0^{X_m(t)} \tilde{W}_i \frac{\partial {}_1}{\partial x}\mathrm{d}x \tag{23}$$

in phase 1, or

$$\int_{X_m(t)}^{1} \tilde{W}_i(x;t)V_2(x;t)\,\mathrm{d}x = \int_{X_m(t)}^{1} \tilde{W}_i \frac{\partial {}_2}{\partial x}\mathrm{d}x \tag{24}$$

in phase 2, and solve for V_1 and V_2, except at the interface where (17) is applied.

3.6.3 The nite element mesh

Having obtained the velocities $V_1(x;t)$ and $V_2(x;t)$, we derive piecewise-linear nodal functions $X_1(x;t); X_2(x;t$x13 0 Td [(cTf 4hosen 4.736oz14i2hensureTJ/ bl80Piil -1f 4y)82(.1.794 T5 Tf88.9552 Tf 4.732W)82(Tf -5.3also -23.9upTf 4.73tTf

,from4-23.9[J8121.9701d-5.3a-44-23.9[J8122.9701d-56 Tld-ste-5.3 Td1(Tf -5.3sa50)]T56 scTf 4hith.1.794 tio.652 Tf52 Tf 4.732Fa

$1(X_1;x;t$ $_1$

0 /F15 1502 0.99-1.9552 Tf 80.10105187.9052.76 T2f 7.031 Tf 14.959 -1.794 Td [(0 /F15 15 11.9552 Tf 4.732 1.794 Td2[(()]1.9552 Tf 4.552 0 Td 7.927167(t)]TJ/F15F6533dt)4126 J/F15 11T-28

3.7 Matrix forms

3.7.1 The velocity potentials

We expand ${}_1(x;t);\ {}_2(x;t)$ in terms of standard piecewise-linear basis functions $W_j(x;t)$ as

$$ {}_1(x;t) = \sum_{j=0}^{m-1} {}_{1;j} W_j(x;t); \qquad {}_2(x;t) = \sum_{j=m+1}^{N+1} {}_{2;j} W_j(x;t) $$

These forms may be substituted into (19) and (20), where $\dot{}_1$ is given by (21) and $\dot{}_2$ by (22), and the resulting systems written in matrix form.

Equations (19) and (20) can then be expressed in the form

$$ \tilde{K}(\underline{U}_1)\,\underline{\ }_1 = \underline{\tilde{f}}_1 \qquad \tilde{K}(\underline{U}_2)\,\underline{\ }_2 = \underline{\tilde{f}}_2 \tag{28} $$

where $\tilde{K}(\underline{U}_1)$, $\tilde{K}(\underline{U}_2)$ are weighted stiffness matrices constructed with the modified basis functions $\tilde{W}_i$, having entries

$$ \int_0^{X_m(t)} U_1(x;t)(\tilde{W}_i)_x (W_j)_x \,\mathrm{d}x; \qquad (i;j = 0;\ldots;m-1); $$

and

$$ \int_{X_m(t)}^{1} U_2(x;t)(\tilde{W}_i)_x (W_j)_x \,\mathrm{d}x; \qquad (i;j = m+1;\ldots;N+1): $$

The vector $\underline{\ }_p$ contains the coefficients ${}_{p;j}$, $(p = 1;2)$, and $\underline{\tilde{f}}_p$, $\underline{\tilde{f}}_p$; are vectors whose entries are the right hand sides of (19),(20), respectively.

Since the matrices $\tilde{K}(\underline{U}_1)$ and $\tilde{K}(\underline{U}_2)$ are both singular (the rows of the left hand sides of both (19) and (20) sum to zero), each of the systems (28) have an infinity of solutions. We set ${}_{p;m} = 0$ at the interface node to obtain unique solutions for ${}_1(x;t)$ and ${}_2(x;t)$. (The rates of change $\dot{}_1$ and $\dot{}_2$ can be found in a straightforward manner by simply summing the rows of equations (28).)

3.7.2 The velocities

In order to derive the velocities we use the expansions

$$ V_1(x;t) = \sum_{j=0}^{m-1} V_{1;j}(t) W_j(x;t); \qquad V_2(x;t) = \sum_{j=m+1}^{N+1} V_{2;j}(t) W_j(x;t) $$

substituted into equation (23) and (24) to obtain

$$\sum_{j=0}^{m\ 1}\left[\int_0^{X_m(t)} \tilde{W}_i W_j \,\mathrm{d}x\right] V_{1;j} = \sum_{j=0}^{m\ 1}\left[\int_0^{X_m(t)} \tilde{W}_i \frac{\partial W_j}{\partial x}\,\mathrm{d}x\right]_{1;j} \tag{29}$$

and

$$\sum_{j=m+1}^{N+1} \int_{X_m(t)}^{1} \tilde{W}_i W_j \,\mathrm{d}x \quad V$$

3. Find the position of the interface node X_m at the next time step from (25) and estimate the interface velocity,

4. Generate the nodal positions $X_{i;j}$, $X_{2;j}$ at the next time-step from $V_{1;j}$, $V_{2;j}$ and the interface velocity, using the explicit Euler scheme,

5. Update the values of $_1$ and $_2$ from $-_1$ and $-_2$ using the same Euler scheme,

6. Find the population densities $\underline{U}_1$ and $\underline{U}_2$ at the next time level by solving equations (34).

4 Results

There is a vast range of parameter values in use because there are so many varied but suitable examples of the type of competition. We select a conservatively representative set of parameters, chosen to demonstrate some of the behaviours that this model is able to describe.

4.1 A parameter choice

Firstly we choose a set of parameters that favour species 1, as shown in figure 2. In this case we see an increasing interface velocity in the initial stages, followed by a long steady phase where the interface velocity is approximately constant (figure 3). As we approach the annihilation of species 2, the interface velocity increases again (figure 4). This is due to the low population of species 2 affecting its ability to grow. The movement of the interface is shown in figure 5.

4.2 Alternative parameter choices

4.2.1 Carrying capacities

We now investigate other parameter choices. We restrict the growth of species 1 by lowering its carrying capacity k_1. We observe that in this scenario neither species is dominant, even though all the competition and diffusion characteristics are uncha7(eter)-22bW5231(is)o F18.7919 -5Tf 81

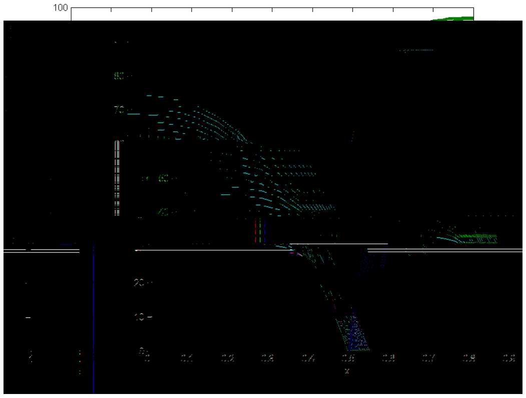

Figure 2: Result of competition model at $t = 1:7$. Here we use $_1 = \;_2 = 0:01$, $k_1 = k_2 = 100$, $r_1 = r_2 = 1$ and 3. We run the model with a time step of $0:0001$ for 17000 steps and plot the results every $0:1$. We see the internal dynamics of the species driving the population densities and interface fluxes, and the position of the interface responding to those fluxes. The initial conditions are shown in red, with species 1 in blue and species 2 in green.

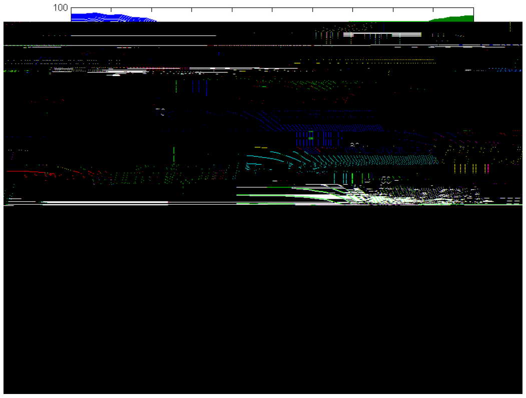

Figure 3: Result of competition model at $t = 6:0$. Here we use $_1 = \;_2 = 0:01$, $k_1 = k_2 = 100$, $r_1 = r_2 = 1$ and = 3. We run the model with a time step of $0:0001$ for 60000 steps and plot the results every $0:1$. The interface continues to evolve and the populations of the species are now limited by the respective carrying capacities. The initial conditions are shown in red, with species 1 in blue and species 2 in green

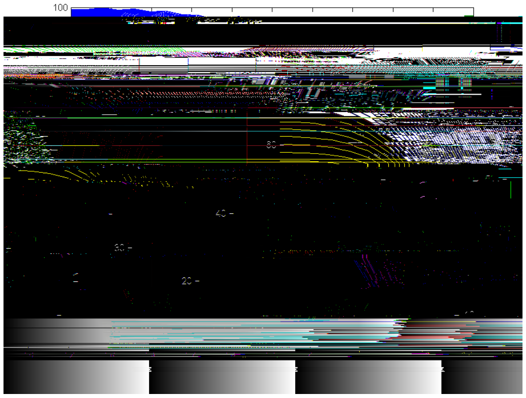

Figure 4: Result of competition model at t = 8:8. Here we use $_1$ = $_2$ = 0:01, k_1 = k_2 = 100, r_1 = r_2 = 1 and = 3. We run the model with a time step of 0:0001 for 88000 steps and plot the results every 0:

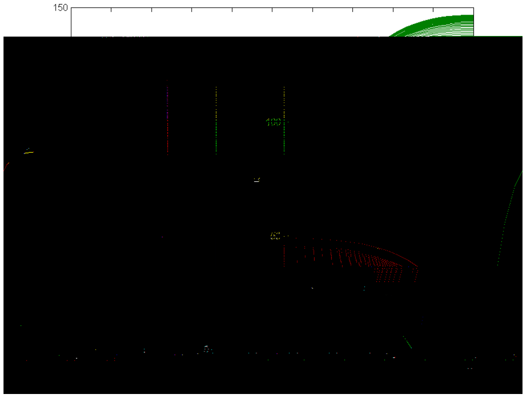

Figure 6: Result of competition model at $t = 8$, considering the effect of altered carrying capacities. Here we use $_1 = {}_2 = 0.01$, $k_1 = 50; k_2 = 150$, $r_1 = r_2 = 1$ and $= 3$. We run the model with a time step of 0.0001 for 80000 steps and plot the results every 0.1. We see that with differently chosen carrying capacities we find the interface position is approximately steady and these two species are in balance.

to make territorial gains due to this property alone (figure 7). However, as time goes on, the growth and competition characteristics become increasingly important. We see species 1 becoming more dominant over time, so that the interface velocity actually reverses direction. Figure 8 shows the evolution of the system at $t = 12.3$, and figure 9 shows the movement of the interface with the direction reversal.

These results give confidence that this model is likely to be able to satisfy the requirements of modelling a wide variety of competition systems. It is stable to a large choice of set-up parameters and is able to produce complex behaviours without problems.

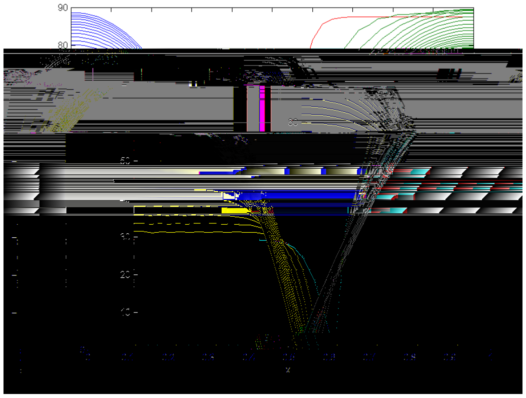

Figure 7: Result of competition model at $t = 3{:}5$, considering the effect of an increased diffusion rate for species 2. Here we use $_1 = 0{:}01;\ _2 = 0{:}05$, $k_1 = k_2 = 100$, $r_1 = r_2 = 1$ and $= 3$. We run the model with a time step of $0{:}0001$ for 35000 steps, and plot the results every $0{:}1$. We observe that species 2 is able to make initial territorial gains due to its high diffusion rate, even though the competition rate is unaltered.

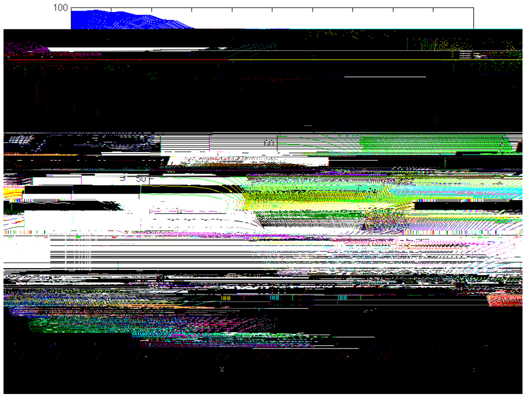

Figure 8: Result of competition model at $t = 12{:}3$, considering the effect of an increased diffusion rate for species 2. Here we use $_1 = 0{:}01;\ _2 = 0{:}05$, $k_1 = k_2 = 100$, $r_1 = r_2 = 1$ and $= 3$. We run the model with a time step of $0{:}0001$ for 123000 iterations, and plot the results every $0{:}1$. We see that the initial diffusion-driven gains by species 2 are reversed, and that the overall growth characteristics are dominating so that species 1 is gaining territory.

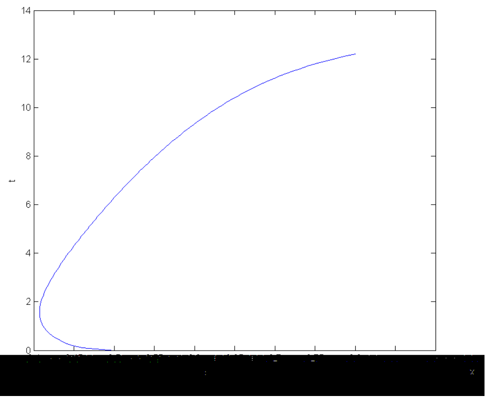

[redacted]

Figure 9: Position of interface, x_m, showing interface movement for the competition model at up to $t = 12.3$, considering the effect of an increased diffusion rate for species 2 (*cf.* figure 5). Here we use $_1 = 0.01;$ $_2 = 0.05$, $k_1 = k_2 = 100$, $r_1 = r_2 = 1$ and $= 3$. We run the model with a time step of 0.0001 for 123000 iterations, and plot the results every 0.1. Due to the growth characteristics we can see interesting temporal effects. Here the interface velocity has actually reversed direction as the system changes from diffusion-dominated to growth-dominated.

5 Summary

In this paper we have applied a moving mesh finite element method based on the relative conservation principle (MMFEM) of [2] to a two-phase Lotka-Volterra competition system with a high competition limit [4], so that the species are completely spatially segregated and interact solely through an interface condition based on this limit.

The model and the MMFEM method are described in detail and the approach implemented for a variety of parameter combinations, observing the various behaviours that dominate as the species evolve through time.

For a set of parameters that favour species 1 we see an increasing interface velocity in the initial stages followed by a long steady phase where the interface velocity is approximately constant. Although the population of species 2 initially grows it is eventually wiped out by the competition with species 1. As the annihilation of species 2 is approached, the interface velocity increases again. The interface continues to evolve and the populations of the species are then limited by the respective carrying capacities. This is due to the low population of species 2 affecting its ability to grow.

If the growth of species 1 is restricted by lowering its carrying capacity we observe that neither species is dominant, even though all the competition and diffusion characteristics are unchanged. Increasing the diffusion rate for species 2, this species is able to make initial territorial gains, even though the competition rate is unaltered. However, as time goes on, growth and competition characteristics become increasingly important so that species 1 becomes more dominant and the interface velocity reverses direction.

A natural extension is to two dimensions along the lines described in [2]: a first attempt appears in reference [6] which foundered only on stability issues. In further work it would be interesting to compare the behaviour of the model

[5] M.E.Hubbard, M.J.Baines, and P.K.Jimack, *Mass-conserving Dirichlet boundary conditions for a moving-mesh finite element algorithm*, Appl. Numer. Math., 59, pp.1337-1353 (2009).

[6] A.R.Watkins, *A Moving Mesh Finite Element Method and its Application to Population Dynamics*, PhD thesis, University of Reading, UK (2017),